

Role of mesonic fluctuations in the Polyakov loop extended quark-meson model at imaginary chemical potential

Kenji Morita,^{1,2} Vladimir Skokov,^{3,*} Bengt Friman,³ and Krzysztof Redlich^{4,2}

¹*Yukawa Institute for Theoretical Physics, Kyoto University, Kyoto 606-8502, Japan*

²*ExtreMe Matter Institute EMMI, GSI, D-64291 Darmstadt, Germany*

³*GSI Helmholtzzentrum für Schwerionenforschung, D-64291 Darmstadt, Germany*

⁴*Institute of Theoretical Physics, University of Wrocław, PL-50204 Wrocław, Poland*

We explore the thermodynamics and phase structure of the Polyakov loop-extended two flavor chiral quark-meson (PQM) model beyond the mean-field approximation at imaginary chemical potential. Our approach is based on the functional renormalization group (FRG) method. At finite temperature and imaginary chemical potential, we solve the renormalization group flow equation for a scale-dependent thermodynamic potential in the presence of the gluonic background field. We determine behavior of order parameters of the PQM model in the FRG approach and compute the phase diagram. We compare our FRG results with that obtained in the mean-field approximation at imaginary chemical potential.

PACS numbers: 12.38.Aw, 12.39.Fe, 25.75.Nq, 05.10.Cc

I. INTRODUCTION

Thermodynamic properties of strongly interacting matter at nonzero baryon density and at finite temperature have been explored numerically within the Lattice Quantum Chromodynamics (LQCD) [1–6]. The LQCD results show that QCD at physical quark masses and at vanishing baryon density exhibits restoration of the chiral symmetry and deconfinement at $T \simeq 160$ MeV [7–9]. The crossover nature of the transition at zero baryon density makes the variation of the order parameters quite smooth and leads to the broader width of the pseudocritical temperature [7].

Unfortunately, the thermodynamics of strongly interacting matter at large baryon densities is presently not accessible in the first principle LQCD calculations, because of a complex structure of fermion determinant. Several methods circumventing this, so-called, sign-problem have been introduced. However, they are limited to small values of chemical potentials or small lattice sizes [10]. Thus, LQCD calculations have not been able yet to address a nature of a critical behavior at finite density on sufficiently large lattices and at small quark masses.

Phenomenological models and effective theories offer a viable framework for exploratory studies. The properties of low-energy hadrons as well as the nature of the chiral phase transition at finite temperature and density have been studied intensively in such effective models [11–30]. Recently, the physics of color confinement and its relation to the chiral symmetry breaking have been also addressed in such a framework. Particularly successful, are models obtained by extending the chiral Lagrangians, such as the Nambu–Jona-Lasinio or the quark-meson, by introduc-

ing a coupling of quarks to uniform temporal background gauge fields, the Polyakov loop [15, 23]. Though, these models have been formulated so as to incorporate essential features of QCD, nevertheless, properties of phase transitions at large baryon densities strongly depend on their parameterizations [18, 23, 25, 31–33].

The imaginary chemical potential formulation provides complementary constraints on the phenomenological models. In addition, at imaginary μ , the phase diagram can be directly computed in LQCD by virtue of the absence of the sign problem. Within LQCD, these results have been used to extrapolate the phase boundary from an imaginary to a real chemical potential [34–39]. Such a strategy was found to be successful in two-color QCD [40], resummed perturbation theory [41], and quasi-particle models [42].

Another interesting issue, that can be addressed at imaginary chemical potential, is the order of the transition at Roberge-Weiss (RW) endpoint, which might dictate the property of the transition at vanishing and finite real chemical potential. Recently, it was shown, within lattice simulations, that the critical behavior at the RW endpoint has a non-trivial dependence on the quark masses for both, two-[43] and three-flavor QCD [44].

The formulation of the theory at imaginary μ also opens the possibility to obtain the canonical partition function from LQCD by means of the Fourier transformation of the grand canonical partition function [45–48]. Therefore, studies of thermodynamics at imaginary chemical potential are important to explore thermodynamics of the QCD at finite density and its phase diagram [49].

The Polyakov loop extended Nambu–Jona-Lasinio (PNJL) [17] and quark-meson (PQM) [23] models reproduce essential features of the QCD thermodynamics already in the mean-field approximation at real and at imaginary chemical potential [50, 51]. Especially, the Roberge-Weiss (RW) periodicity $Z(\mu_I/T) = Z(\mu_I/T +$

*E-Mail: V.Skokov@gsi.de

$2\pi k/N_c$) and the associated $Z(N_c)$ transition at high temperature [52] can be described in these models.

In our previous studies [51], we have discussed the phase structure of the PNJL model at imaginary chemical potential. While the statistical confinement feature of this model naturally provides characteristic properties of the order parameters, the chiral condensate and the Polyakov loop, its thermodynamics, however, is strongly influenced by the choice of the Polyakov loop potential. Furthermore, to reproduce within the mean field approximation the LQCD results in terms of such effective models, several amendments seem to be necessary [28, 53–55].

To correctly account for the critical behavior and scaling properties near the chiral phase transition, it is necessary to go beyond the mean-field approximation and include fluctuations and non-perturbative dynamics. This can be achieved e.g. by using methods based on the functional renormalization group (FRG) [56–61].

In the following, we consider the PQM model at imaginary chemical potential and study its critical properties and phase diagram within FRG approach. We formulate and solve the suitably truncated FRG flow equation for fluctuations of the meson fields in the presence of the Polyakov loop which is treated as a background field on the mean-field level. We extend previous studies [62] to imaginary chemical potential and explore influence of fluctuations on the chiral and deconfinement order parameters. We compare our FRG results at imaginary chemical potential with that obtained in the mean field approximation. We show, that there is an essential modification of thermodynamics at imaginary chemical potential owing to quantum mesonic fluctuations.

The FRG approach was previously applied to study the phase structure of two-flavor QCD in the chiral limit at imaginary chemical potential [49]. In the current paper, we perform calculations within the PQM model to study the role of the mesonic fluctuations on the structure of the phase diagram at imaginary chemical potential by comparing results obtained within the FRG approach and under the mean-field approximation.

In the next section, we introduce the PQM model and the implementation of the FRG method at imaginary μ . We present our results in Sec. III. Section IV is devoted to the summary.

II. THE POLYAKOV-QUARK-MESON MODEL

The quark–meson model is an effective realization of the low–energy sector of QCD, which incorporates chiral symmetry. Because the local color $SU_c(N)$ invariance of QCD is replaced by a global symmetry, the model does not describe confinement. Nevertheless, by introducing a coupling of the quarks to a uniform temporal color gauge field, represented by the Polyakov loop, some confinement properties can be effectively included [15, 22, 23].

The Lagrangian of the PQM model reads [23]

$$\mathcal{L} = \bar{q} [i\gamma^\nu D_\nu - g(\sigma + i\gamma_5 \vec{\tau} \cdot \vec{\pi})] q + \frac{1}{2}(\partial_\nu \sigma)^2 + \frac{1}{2}(\partial_\nu \vec{\pi})^2 - U(\sigma, \vec{\pi}) - \mathcal{U}(\Phi, \Phi^*). \quad (1)$$

The coupling between the effective gluon field and quarks is implemented through the covariant derivative

$$D_\nu = \partial_\nu - iA_\nu, \quad (2)$$

where $A_\nu = g A_\nu^a \lambda^a / 2$. The spatial components of the gluon field are neglected, i.e. $A_\nu = \delta_{\nu 0} A_0$. Moreover, $\mathcal{U}(\Phi, \Phi^*)$ is the effective potential for the gluon field expressed in terms of the thermal expectation values of the color trace of the Polyakov loop and its conjugate

$$\Phi = \frac{1}{N_c} \langle \text{Tr}_c L(\vec{x}) \rangle, \quad \Phi^* = \frac{1}{N_c} \langle \text{Tr}_c L^\dagger(\vec{x}) \rangle, \quad (3)$$

with

$$L(\vec{x}) = \mathcal{P} \exp \left[i \int_0^\beta d\tau A_4(\vec{x}, \tau) \right], \quad (4)$$

where \mathcal{P} stands for the path ordering, $\beta = 1/T$ and $A_4 = iA_0$. In the $O(4)$ representation, the meson field is introduced as $\phi_m = (\sigma, \vec{\pi})$ and the corresponding $SU(2)_L \otimes SU(2)_R$ chiral representation is defined by $\sigma + i\vec{\tau} \cdot \vec{\pi} \gamma_5$.

The purely mesonic potential of the model $U(\sigma, \vec{\pi})$, is defined as

$$U(\sigma, \vec{\pi}) = \frac{\lambda}{4} (\sigma^2 + \vec{\pi}^2 - v^2)^2 - c\sigma, \quad (5)$$

while the effective potential of the gluon field is parametrized in such a way as to preserve the $Z(3)$ invariance,

$$\frac{\mathcal{U}(\Phi, \Phi^*)}{T^4} = -\frac{b_2(T)}{2} \Phi^* \Phi - \frac{b_3}{6} (\Phi^3 + \Phi^{*3}) + \frac{b_4}{4} (\Phi^* \Phi)^2. \quad (6)$$

The parameters,

$$b_2(T) = a_0 + a_1 \left(\frac{T_0}{T} \right) + a_2 \left(\frac{T_0}{T} \right)^2 + a_3 \left(\frac{T_0}{T} \right)^3 \quad (7)$$

with $a_0 = 6.75$, $a_1 = -1.95$, $a_2 = 2.625$, $a_3 = -7.44$, $b_3 = 0.75$, $b_4 = 7.5$ and $T_0 = 270$ MeV were chosen to reproduce the equation of state of the pure $SU_c(3)$ lattice gauge theory. When the coupling to the quark degrees of freedom are neglected, the potential (6) yields a first-order deconfinement phase transition at T_0 .

Alternative parametrization of the Polyakov loop potential, see e.g. Ref. [32], may provide a better fit of the lattice results by the PQM model. However, we follow our previous studies of the PQM model formulated at the real chemical potential, and apply the potential (6) in the model calculations at imaginary μ . The main conclusions on the influence of the mesonic fluctuations on the phase structure will not change if different parametrization of the potential is considered.

A. The FRG method in the PQM model

In order to account for mesonic fluctuations in the PQM model, we employ a scheme based on the functional renormalization group (FRG). This scheme involves an infrared regularization of the fluctuations at a sliding

momentum scale k , resulting in a scale-dependent effective action Γ_k , the so-called effective average action [56–59]. We treat the Polyakov loop as a background field, which is introduced self-consistently on the mean-field level while fluctuations of the quark and meson fields are accounted for by solving the FRG flow equations.

Following our previous work [62], we formulate the flow equation for the scale-dependent grand canonical potential density $\Omega_k = T\Gamma_k/V$ for the quark and meson subsystems at finite temperature T and imaginary chemical potential $\mu = i\theta T$ as follows

$$\begin{aligned} \partial_k \Omega_k(\Phi, \Phi^*; T, \theta) = & \frac{k^4}{12\pi^2} \left\{ \frac{3}{E_\pi} \left[1 + 2n_B(E_\pi; T) \right] + \frac{1}{E_\sigma} \left[1 + 2n_B(E_\sigma; T) \right] \right. \\ & \left. - \frac{4N_c N_f}{E_q} \left[1 - N(\Phi, \Phi^*; T, \theta) - \bar{N}(\Phi, \Phi^*; T, \theta) \right] \right\}. \end{aligned} \quad (8)$$

Here $n_B(E_{\pi,\sigma}; T)$ is the bosonic distribution function

$$n_B(E_{\pi,\sigma}; T) = \frac{1}{\exp(\beta E_{\pi,\sigma}) - 1}$$

with the pion and sigma energies

$$E_\pi = \sqrt{k^2 + \bar{\Omega}'_k}, \quad E_\sigma = \sqrt{k^2 + \bar{\Omega}'_k + 2\rho \bar{\Omega}''_k},$$

where the primes denote derivatives of $\bar{\Omega} = \Omega + c\sigma$ with respect to ρ field, $\rho = (\sigma^2 + \vec{\pi}^2)/2$, and $\beta = 1/T$. The fermion distribution functions $N(\Phi, \Phi^*; T, \theta)$ and $\bar{N}(\Phi, \Phi^*; T, \theta)$,

$$N(\Phi, \Phi^*; T, \theta) = \frac{1 + 2\Phi^* \exp[\beta E_q - i\theta] + \Phi \exp[2(\beta E_q - i\theta)]}{1 + 3\Phi \exp[2(\beta E_q - i\theta)] + 3\Phi^* \exp[\beta E_q - i\theta] + \exp[3(\beta E_q - i\theta)]}, \quad (9)$$

$$\bar{N}(\Phi, \Phi^*; T, \theta) = N(\Phi^*, \Phi; T, -\theta), \quad (10)$$

are modified because of the coupling to the gluon field. Finally, the quark energy is given by

$$E_q = \sqrt{k^2 + 2g^2\rho}. \quad (11)$$

The minimum of the thermodynamic potential is determined by the stationarity condition

$$\left. \frac{d\Omega_k}{d\sigma} \right|_{\sigma=\sigma_k} = \left. \frac{d\bar{\Omega}_k}{d\sigma} \right|_{\sigma=\sigma_k} - c = 0. \quad (12)$$

The flow equation (8) is solved numerically with the initial cutoff $\Lambda = 1.2$ GeV (see details in Ref. [62]). The initial conditions for the flow are chosen to reproduce the in-vacuum properties: the physical pion mass $m_\pi = 138$ MeV, the pion decay constant $f_\pi = 93$ MeV, the sigma mass $m_\sigma = 600$ MeV, and the constituent quark mass $m_q = 300$ MeV at the scale $k \rightarrow 0$. The symmetry breaking term, $c = m_\pi^2 f_\pi$, corresponds to an external field and consequently does not flow. In this work, we neglect the flow of the Yukawa coupling g , which is not expected to be significant for the present studies (see e.g. Refs. [65, 66]).

By solving the equation (8), one obtains the thermodynamic potential for the quark and mesonic subsystems, $\Omega_{k \rightarrow 0}(\Phi, \Phi^*; T, \theta)$, as a function of the Polyakov loop variables Φ and Φ^* . The full thermodynamic potential $\Omega(\Phi, \Phi^*; T, \theta)$ in the PQM model, including quark, meson and gluon degrees of freedom, is obtained by adding the effective gluon potential $\mathcal{U}(\Phi, \Phi^*)$ to $\Omega_{k \rightarrow 0}(\Phi, \Phi^*; T, \theta)$:

$$\Omega(\Phi, \Phi^*; T, \theta) = \Omega_{k \rightarrow 0}(\Phi, \Phi^*; T, \theta) + \mathcal{U}(\Phi, \Phi^*). \quad (13)$$

At a given temperature and chemical potential, the Polyakov loop variables, Φ and Φ^* , are then determined by the stationarity conditions:

$$\frac{\partial}{\partial \Phi} \Omega(\Phi, \Phi^*; T, \theta) = 0, \quad (14)$$

$$\frac{\partial}{\partial \Phi^*} \Omega(\Phi, \Phi^*; T, \theta) = 0. \quad (15)$$

The thermodynamic potential (13) does not contain contributions of thermal modes with momenta larger than the cutoff Λ . We take into account the contribu-

tion of the high momentum states by approximating it as quarks interacting only with Polyakov loop degrees of freedom as done in Ref. [62].

B. The mean-field approximation

To show the importance of mesonic fluctuations on the thermodynamics of the PQM model formulated at imaginary μ we compare the FRG results with those obtained in the mean-field approximation. In the latter, mesonic fluctuations are neglected and the mesonic fields are replaced by their classical expectation values.

The thermodynamical potential of the PQM model in the mean-field approximation reads [23],

$$\Omega_{\text{MF}} = \mathcal{U}(\Phi, \Phi^*) + U(\langle\sigma\rangle, \langle\pi\rangle = 0) + \Omega_{q\bar{q}}(\langle\sigma\rangle, \Phi, \Phi^*). \quad (16)$$

Here, the contribution of quarks with the dynamical mass $m_q = g\langle\sigma\rangle$ is given by

$$\Omega_{q\bar{q}}(\langle\sigma\rangle, \Phi, \Phi^*) = -\frac{N_c N_f}{8\pi^2} m_q^4 \ln\left(\frac{m_q}{M}\right) - 2N_f T \int \frac{d^3p}{(2\pi)^3} \left\{ \ln g^{(+)}(\langle\sigma\rangle, \Phi, \Phi^*; T, \theta) + \ln g^{(-)}(\langle\sigma\rangle, \Phi, \Phi^*; T, \theta) \right\}, \quad (17)$$

where

$$g^{(+)}(\langle\sigma\rangle, \Phi, \Phi^*; T, \theta) = 1 + 3\Phi \exp[-(\beta E_q - i\theta)] + 3\Phi^* \exp[-2(\beta E_q - i\theta)] + \exp[-3(\beta E_q - i\theta)], \quad (18)$$

$$g^{(-)}(\langle\sigma\rangle, \Phi, \Phi^*; T, \theta) = g^{(+)}(\langle\sigma\rangle, \Phi^*, \Phi; T, -\theta) \quad (19)$$

and $E_q = \sqrt{p^2 + m_q^2}$ is the quark quasi-particle energy. The first term in Eq. (17) is a vacuum contribution regularized by dimensional regularization with renormalization scale M [67]. The relevance of the vacuum contribution for the thermodynamics of chiral models was demonstrated and studied in detail in Refs. [67] and [68].

The equations of motion for the mean fields are obtained by requiring that the thermodynamic potential is stationary with respect to changes of $\langle\sigma\rangle$, Φ and Φ^* . Utilizing the fact that Φ^* is the complex conjugate of Φ at imaginary chemical potential, we introduce the modulus and the phase of the Polyakov loop as $\Phi = |\Phi|e^{i\phi}$ and $\Phi^* = |\Phi|e^{-i\phi}$ and the stationary condition is given as

$$\frac{\partial\Omega_{\text{MF}}}{\partial\langle\sigma\rangle} = \frac{\partial\Omega_{\text{MF}}}{\partial|\Phi|} = \frac{\partial\Omega_{\text{MF}}}{\partial\phi} = 0. \quad (20)$$

The model parameters are fixed to reproduce the same vacuum physics as in the FRG calculation.

III. THERMODYNAMICS OF THE PQM MODEL

The PQM model, which is expected to belong to the same universality class as QCD, exhibits a generic phase diagram with a critical point at a non-vanishing real chemical potential [23]. A detailed comparison between thermodynamic properties of the PQM model obtained within the FRG and in the mean-field approach at real chemical potential was recently studied in Ref. [69].

In the following, we explore the critical properties of the PQM model at imaginary chemical potential $\mu/T =$

$-i\theta$ using the functional renormalization group approach and in the mean-field approximation.

Under the mean-field dynamics, many features of the PQM model at imaginary chemical potential should be common with that obtained previously in the PNJL model. Thus, the nature of the phase structure in the mean-field approximation for the PNJL model found in Ref. [51] also applies to our present calculations within the PQM model. Therefore, we focus on the effects of the mesonic fluctuations on thermodynamics at imaginary chemical potential and at finite temperature.

At imaginary chemical potential, in addition to the chiral transition which is characterized by the chiral order parameter σ and the deconfinement transition which is indicated by the rapid increase of the modulus of the Polyakov loop, the PQM model exhibits also the Roberge-Weiss (RW) transition. Since the thermodynamic potential of the PQM model shares the Roberge-Weiss periodicity of QCD, $\Omega(T, \theta) = \Omega(T, \theta + \frac{2\pi n}{3})$ with $n \in \mathbb{Z}$, which is a remnant of global $Z(3)$ symmetry of the $SU_c(3)$ gauge group, the first-order RW phase transition takes place in the deconfined phase at $\theta = \pi/3$. The RW transition can be understood as a sudden change of the phase ϕ of the Polyakov loop. While ϕ as a function of θ smoothly changes below the RW endpoint, at $T = T_{\text{RW}}$ it has a discontinuity caused by a transition from one $Z(3)$ sector to another. This transition also influences the thermodynamic potential and the modulus of the Polyakov loop as a cusp at $\theta = \pi/3$. Therefore, at imaginary chemical potential, the model contains three variables; σ , $|\Phi|$, and the phase ϕ as the order parameters for the corresponding phase transitions.

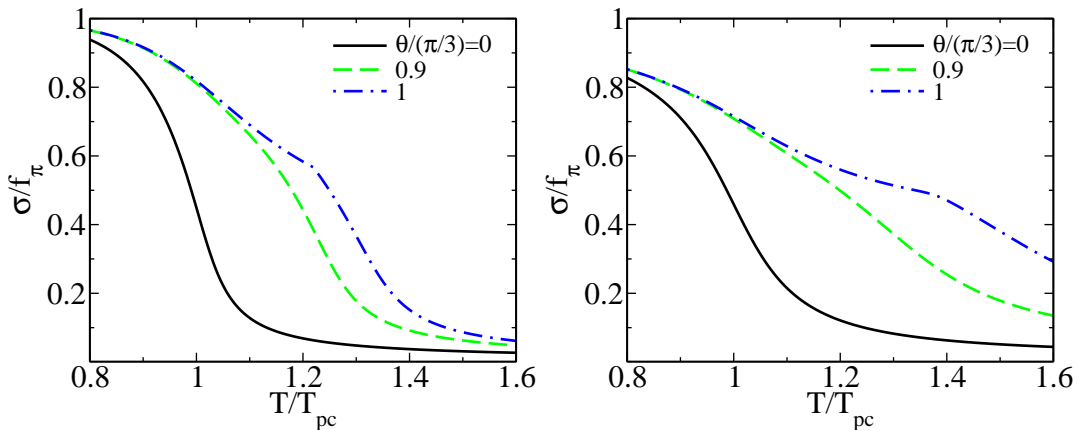


FIG. 1: The chiral order parameter normalized by f_π , as a function of temperature for different values of θ for the PQM model in the mean-field approximation (left panel) and in the FRG approach (right panel).

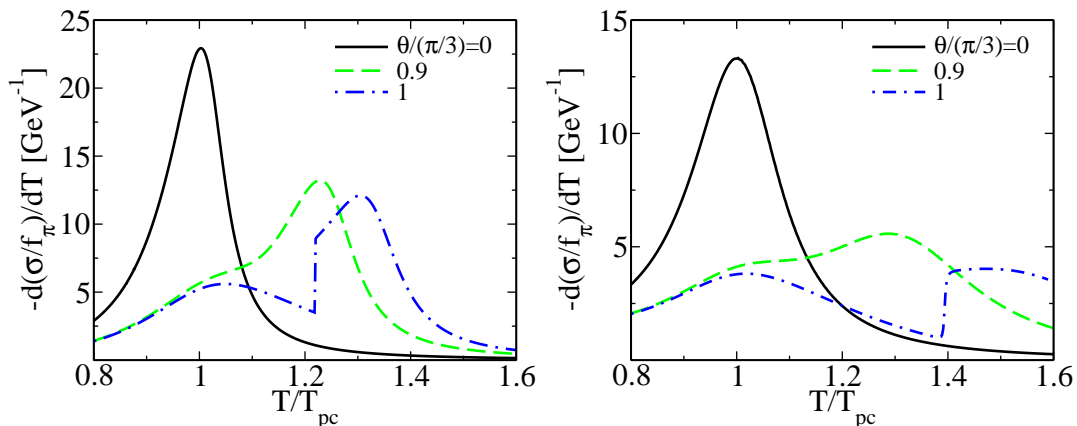


FIG. 2: The temperature derivative of the chiral order parameter as a function of temperature for different values of θ for the PQM model in the mean-field approximation (left panel) and in the FRG approach (right panel).

A. Properties of order parameters in the presence of mesonic fluctuations

By solving the flow equation (8) for the quantum potential we can calculate properties of all three order parameters discussed above in the presence of mesonic fluctuations.

Figure 1 shows the chiral order parameter normalized by $f_\pi = 93$ MeV as a function of temperature scaled by the chiral crossover temperature at $\theta = 0$, T_{pc} . To identify T_{pc} the maximum of $-\sigma/dT$ was used.

The order parameter is shown in Fig. 1 for various values of the imaginary chemical potential. The FRG results are compared to that obtained in the mean-field approximation. There is a clear change in the shape of σ with increasing θ from 0 to $\theta = \pi/3$. This is the case in the mean-field as well as in the FRG approach. However, the mesonic fluctuations included in the FRG scheme imply a strong smearing of the order parameter, making the chiral transition smoother. This effect is even more pronounced in the derivative of the order parameter with

respect to the temperature. As seen in Fig. 2 the peak value of $-d(\sigma/f_\pi)/dT$ in the FRG calculations at vanishing chemical potential is almost a half of the mean field counterpart. From Fig. 2 one also sees, that in the mean-field as well as in the FRG calculations, the peak of $-d(\sigma/f_\pi)/dT$ shifts to higher temperature with increasing θ . Applying an analytical continuation such a shift was used to describe the change of the chiral cross over transition temperature with real chemical potential [34].

In the present calculation, however, one sees two peaks structure in $-d(\sigma/f_\pi)/dT$. The ones at higher temperature are associated with the chiral crossover transition, as it is smoothly connected from the unique peak at small θ . The first peak, which is due to the deconfinement transition, was not previously observed in the mean-field calculations in the PNJL model. Its presence in the PQM model has to be attributed to the specific implementation of the chiral sector. The discontinuity which is specific to $\theta = \pi/3$, appears at $T = 1.22 T_{pc}$ in the mean field and at $T = 1.39 T_{pc}$ in the FRG calculations. This discontinuity is attributable to the RW endpoint where the phase ϕ

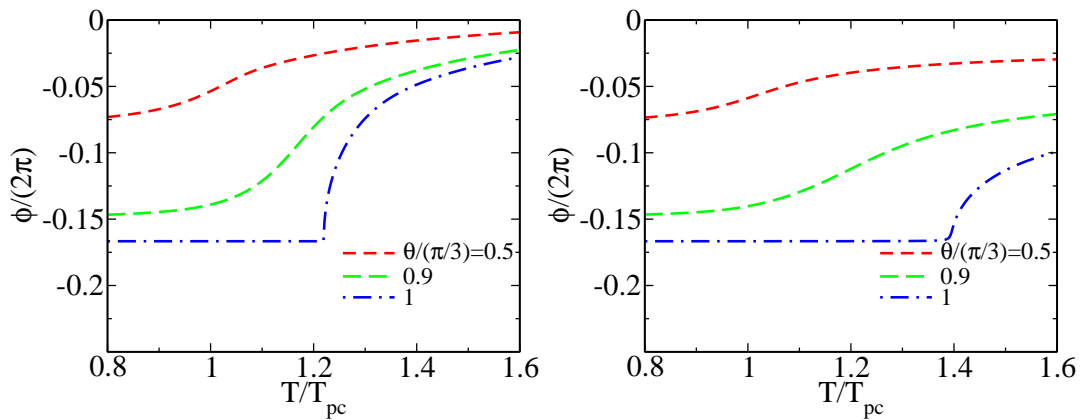


FIG. 3: The phase of the Polyakov loop ϕ as a function of temperature for different values of θ for the PQM model in the mean-field approximation (left panel) and in the FRG approach (right panel).

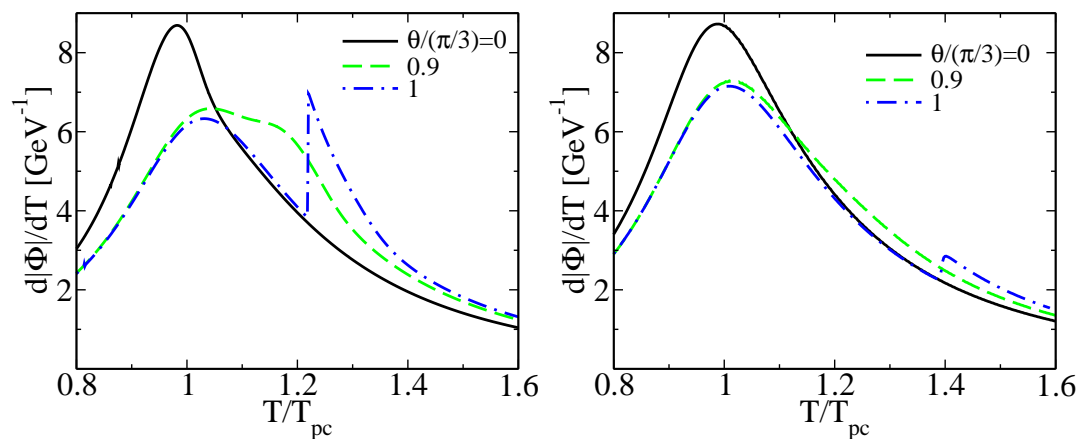


FIG. 4: The temperature derivative of modulus of the Polyakov loop as a function of temperature for different values of θ for the PQM model in the mean-field approximation (left panel) and in the FRG approach (right panel).

of the Polyakov loop shows a critical behavior. We note, that in the LGT calculations, the RW end point is located at $T \approx (1.1 - 1.2)T_{pc}$ [36]. The obtained model results on this temperature strongly depend on the parametrization of the Polyakov loop potential. For instance, for the logarithmic potential [32], the discontinuity of $-d(\sigma/f_\pi)/dT$ at $\theta = \pi/3$ appears at $T = 1.08T_{pc}$ for the FRG approach and $T = 1.09T_{pc}$ in the mean-field approximation.

Figure 3 shows the ϕ as a function of temperature.¹ We find in the PQM model with the polynomial potential (6) the second-order transition both in the FRG approach and in the mean-field approximation. Thus, the RW endpoint is a critical point located at $\theta = \pi/3 + 2\pi n/3$ and at $T_{RW}/T_{pc} = 1.39$ in the FRG approach and at a lower temperature $T_{RW}/T_{pc} = 1.22$ in the mean-field approximation. Although the order of the transition remains

unchanged by the fluctuations, in the FRG calculations the $\phi(T)$ is a smoother function of temperature. The Polyakov loop is treated within the mean-field approximation also in the FRG approach, thus the observed smoothing of $\phi(T)$ in Fig. 3 (right) appears owing to its coupling to the chiral order parameter which is smeared by the quantum fluctuations.

The effect of the fluctuations on the deconfinement transition is more transparent if the derivative of $|\Phi|$ with respect to the temperature is considered. The $d|\Phi|/dT$ as a function of T is depicted in Fig. 4 in the FRG and mean-field calculations. At small θ this derivative has a unique peak, that is attributed to the location of the deconfinement transition. However, near $\theta = \pi/3$, where the phase ϕ also changes rapidly, an additional peak appears. In the mean-field calculations one sees two well-separated maxima. At $\theta = \pi/3$, where the second-order RW endpoint appears as the rapid change of ϕ seen in Fig. 3, there is a discontinuity in $d|\Phi|/dT$ at $T = T_{RW}$, both in the mean-field and in the FRG calculations. However, the jump associated with the RW endpoint is smaller in the FRG case. This, as shown in Figs. 1 and 3, is due to mesonic

¹ $\theta = \pi/3$ above T_{RW} is the first-order transition line where two minima coexist and T_{RW} is the bifurcation. For simplicity in the figure, we omit the other minimum in ϕ .

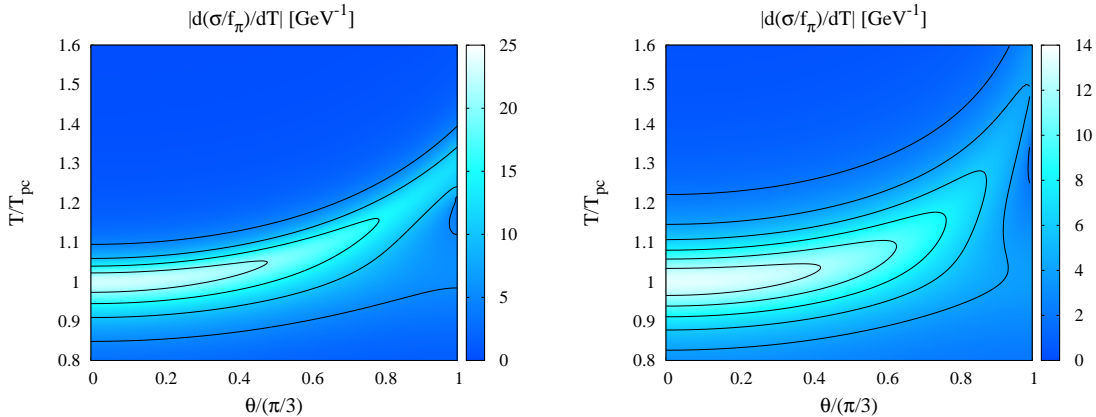


FIG. 5: Contour plots of the temperature derivative of modulus of the chiral order parameter in the mean-field approximation (left panel) and in the FRG approach (right panel).

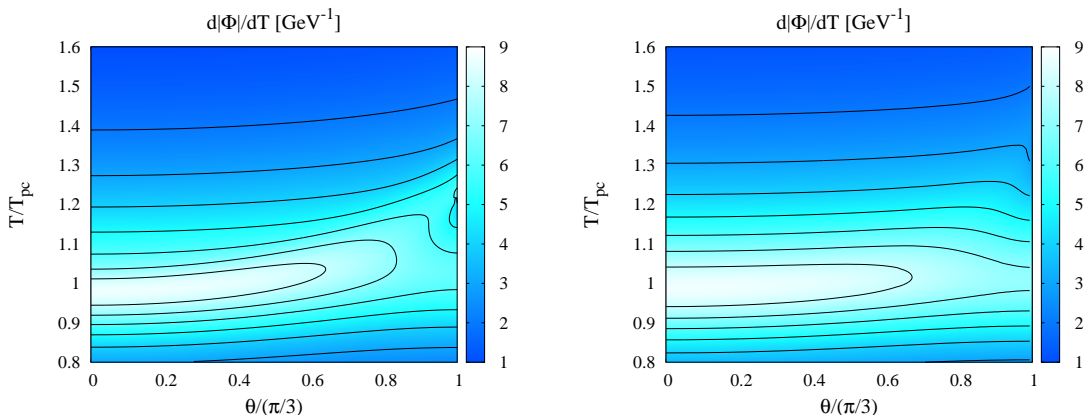


FIG. 6: Contour plots of the temperature derivative of the modulus of the Polyakov loop in the mean-field approximation (left panel) and in the FRG approach (right panel).

fluctuations which smoothen the critical behavior of the chiral order parameter and the phase ϕ . Consequently, as seen in Fig. 4 (right), the discontinuity of $d|\Phi|/dT$ at $\theta = \pi/3$ induced by the RW endpoint becomes weaker. Nevertheless, in these studies, the deconfinement transition, defined by the peak of $d|\Phi|/dT$, is now separated from the RW transition contrary to previous analysis in the PNJL model [50, 51]. One should note, however, that such separation occurs only in the case of the polynomial Polyakov loop potential (6), which violates the restriction on the Polyakov loop target space required by the $SU(3)$ Haar measure [51]. If one uses the logarithmic potential [32] which exhibits stronger transition, the deconfinement critical line connects to the RW endpoint, as expected.

B. Phase diagrams

The properties of order parameters in the PQM model discussed above, can be also represented as the phase di-

agram in the $(T - \theta)$ plane. For illustration, we show in Figs. 5 and 6 contour maps of $-d(\sigma/f_\pi)/dT$ for the chiral transition and $d|\Phi|/dT$ for the deconfinement. The effect of fluctuations can be clearly seen in the changes of the contours. The crossover chiral line, defined by the maximum of $-d(\sigma/f_\pi)/dT$, meets the first-order RW transition at $T_{ce}/T_{pc} = 1.47$ if the fluctuations are included, and at $T_{ce}/T_{pc} = 1.30$ in the mean-field approximation. However, as discussed above, at imaginary chemical potential, the transition points for the chiral and deconfinement crossover are not determined unambiguously as they depend on the particular choice of the Polyakov loop potential. In the present calculations, the double peak structure can be read off from the contour maps.

An alternative determination of the chiral critical line is based on the location of the minimum in the sigma meson mass m_σ . Figure 7 shows the contour maps for m_σ , normalized to its vacuum value m_σ^0 . One sees in this figure that the double peak structure induced by the deconfinement does not show up in the sigma mass. The effect of fluctuations appears as a smearing of the sharp

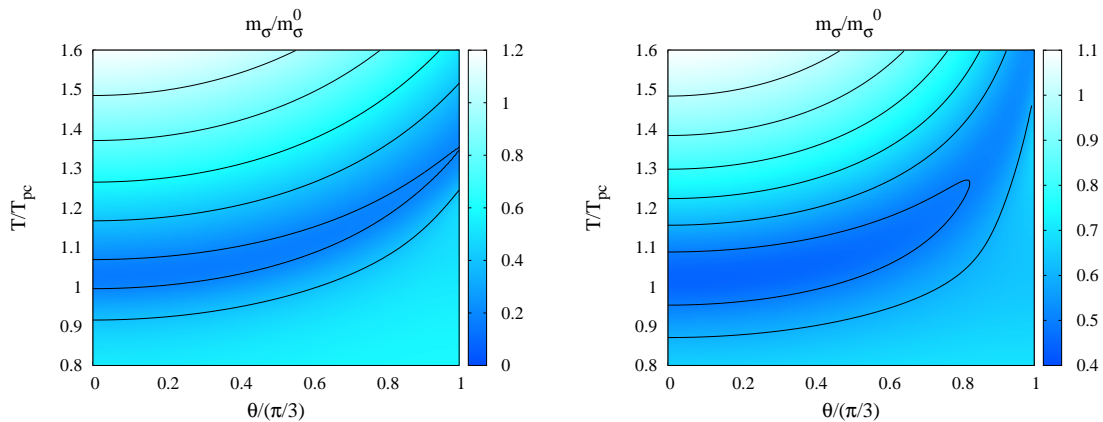


FIG. 7: Contour plots of the sigma mass in the mean-field approximation (left panel) and in the FRG approach (right panel).

minimum and the stronger curvature. This is evident in Fig. 7 when comparing results obtained in the mean-field approximation (left) with the FRG approach (right).

IV. SUMMARY AND CONCLUSIONS

We have formulated and explored the thermodynamics of the Polyakov loop extended quark–meson model (PQM) at imaginary chemical potential, including mesonic fluctuations within the functional renormalization group method (FRG). The flow equations for the scale-dependent thermodynamic potential at finite temperature and at imaginary chemical potential were solved in the presence of a background gluonic field.

We have shown that the non-perturbative fluctuations included in the FRG approach have an important effect on the critical properties of the system. Specifically, the fluctuations smoothen the chiral phase transition. We find that this leads to modification of the curvature of the chiral critical line. We also find that the Polyakov loop variables (modulus and phase) are also smeared by fluctu-

ations of the chiral order parameter. We point out that the deconfinement crossover transition and the second-order Roberge-Weiss endpoint can be separated if the polynomial Polyakov loop effective potential is used to model the gluon thermodynamics.

Our results show, that fluctuations of the meson field and non-perturbative effects have to be included when studying critical behavior of effective chiral models. Such fluctuations can modify substantially the model properties and predictions. This is particularly important when one attempts to quantify lattice QCD results within effective chiral models.

Acknowledgments

V. Skokov acknowledges the support by the Frankfurt Institute for Advanced Studies (FIAS). K. Morita is supported by the Yukawa International Program for Quark-Hadron Sciences (YIPQS) at Kyoto University. K. Redlich acknowledges partial support by the Polish Ministry of Science.

-
- [1] Z. Fodor, and S. D. Katz, *Phys.Lett. B* **534**, 87 (2002).
 - [2] C. R. Allton, S. Ejiri, S. J. Hands, O. Kaczmarek, F. Karsch, E. Laermann, and C. Schmidt, *Phys. Rev. D* **68**, 014507 (2003).
 - [3] C. R. Allton, M. Doring, S. Ejiri, S.J. Hands, O. Kaczmarek, F. Karsch, E. Laermann, and K. Redlich, *Phys. Rev. D* **71**, 054508 (2005).
 - [4] S. Muroya, A. Nakamura, C. Nonaka, and T. Takaishi, *Prog. Theor. Phys.* **110**, 615 (2003).
 - [5] O. Kaczmarek, F. Karsch, E. Laermann, C. Miao, S. Mukherjee, P. Petreczky, C. Schmidt, W. Soeldner, and W. Unger, *Phys. Rev. D* **83**, 014504 (2011).
 - [6] G. Endrodi, Z. Fodor, S. D. Katz, K. K. Szabo, *JHEP* **1104**, 001 (2011).
 - [7] Y. Aoki, G. Endrödi, Z. Fodor, S. D. Katz, and K. K. Szabo, *Nature* **443** (2006) 675.
 - [8] S. Borsányi, Z. Fodor, C. Hoelbling, S. D. Katz, S. Krieg, C. Ratti, and K. K. Szabo, *JHEP* **1009**, 073 (2010).
 - [9] A. Bazavov and P. Petreczky (HotQCD Collaboration), arXiv:1107.5027.
 - [10] P. de Forcrand, *PoS LAT2009*,010 (2009).
 - [11] A. Gocksch and M. Ogilvie, *Phys. Rev. D* **31**, 877 (1985).
 - [12] T. Hatsuda and T. Kunihiro, *Phys. Rept.* **247**, 221 (1994).
 - [13] M. Buballa, *Phys. Rept.* **407**, 205 (2005).
 - [14] P. N. Meisinger and M. C. Ogilvie, *Phys. Lett. B* **379**, 163 (1996). P. N. Meisinger, T. R. Miller and M. C. Ogilvie, *Phys. Rev. D* **65**, 034009 (2002).
 - [15] K. Fukushima, *Phys. Lett. B* **591**, 277 (2004).
 - [16] F. Sannino, *Phys. Rev. D* **66**, 034013 (2002); A. Mócsy, F. Sannino and K. Tuominen, *Phys. Rev. Lett.* **92**, 182302 (2004).

- [17] C. Ratti, M. A. Thaler and W. Weise, Phys. Rev. D **73**, 014019 (2006).
- [18] C. Sasaki, B. Friman and K. Redlich, Phys. Rev. D **77**, 034024 (2008); Phys. Rev. Lett. **99**, 232301 (2007); Phys. Rev. D **75**, 074013 (2007).
- [19] S. Digal, E. Laermann and H. Satz, Eur. Phys. J. C **18**, 583 (2001).
- [20] E. Megias, E. Ruiz Arriola and L. L. Salcedo, Phys. Rev. D **74**, 065005 (2006).
- [21] E. M. Ilgenfritz and J. Kripfganz, Z. Phys. C **29**, 79 (1985).
- [22] K. Fukushima, Phys. Lett. B **553**, 38 (2003); Phys. Rev. D **68**, 045004 (2003).
- [23] B. J. Schaefer, J. M. Pawłowski and J. Wambach, Phys. Rev. D **76**, 074023 (2007).
- [24] C. Sasaki and I. Mishustin, Phys. Rev. C **82**, 035204 (2010); C. Sasaki, Acta. Phys. Polon. Supp. **3**, 659 (2010); M. Harada, C. Sasaki and S. Takemoto, Phys. Rev. D **81** (2010) 016009.
- [25] H. Abuki, R. Anglani, R. Gatto, G. Nardulli, and M. Ruggieri, Phys. Rev. D **78**, 034034 (2008).
- [26] T. Kahara and K. Tuominen, Phys. Rev. D **82** 114026, (2010).
- [27] L. F. Palhares and E. S. Fraga, Phys. Rev. D **82**, 125018 (2010).
- [28] Y. Sakai, T. Sasaki, H. Kouno, and M. Yahiro, Phys. Rev. D **82**, 076003 (2010).
- [29] D. Horvatić, D. Blaschke, D. Klabučar, and O. Kaczmarek, arXiv:1012.2113.
- [30] G. Aarts, S. P. Kumar, and J. Rafferty, JHEP **1007**, 056 (2010).
- [31] M. A. Stephanov, PoS **LAT2006**, 024 (2006).
- [32] C. Ratti, S. Roessner and W. Weise, Phys. Lett. B **649**, 57 (2007); S. Roessner, C. Ratti, and W. Weise, Phys. Rev. D **75**, 034007 (2007).
- [33] E. S. Bowman and J. I. Kapusta, Phys. Rev. C **79**, 015202 (2009).
- [34] P. de Forcrand and O. Philipsen, Nucl. Phys. **B642**, 290 (2002); *ibid.* **B673**, 170 (2003).
- [35] P. de Forcrand and O. Philipsen, JHEP **0701**, 077 (2007).
- [36] M. D'Elia and M. P. Lombardo, Phys. Rev. D **67**, 014505 (2003); *ibid.* **70**, 074509 (2004).
- [37] L. K. Wu, X. Q. Luo, and H. S. Chen, Phys. Rev. D **76**, 034505 (2007).
- [38] P. Cea, L. Cosmai, M. D'Elia, and A. Papa, Phys. Rev. D **81**, 094502 (2010).
- [39] K. Nagata and A. Nakamura, Phys. Rev. D **83**, 114507 (2011).
- [40] P. Giudice and A. Papa, Phys. Rev. D **69**, 094509 (2004); P. Cea, L. Cosmai, M. D'Elia, C. Manneschi, and A. Papa, *ibid.* **80**, 034501 (2009).
- [41] A. Hart, M. Laine, and O. Philipsen, Phys. Lett. B **505**, 141 (2001).
- [42] M. Bluhm and B. Kämpfer, Phys. Rev. D **77**, 034004 (2008).
- [43] C. Bonati, G. Cossu, M. D'Elia, and F. Sanfilippo, Phys. Rev. D **83**, 054505 (2011).
- [44] P. de Forcrand and O. Philipsen, Phys. Rev. Lett. **105**, 152001 (2010).
- [45] M. Alford, A. Kapustin, and F. Wilczek, Phys. Rev. D **59**, 054502 (1999).
- [46] F. de Forcrand and S. Kratochvila, Nucl. Phys. B (Proc. Suppl.) **153**, 62 (2006).
- [47] S. Ejiri, Phys. Rev. D **78**, 074507 (2008).
- [48] A. Li, A. Alexandru, K. F. Liu, and X. Meng, Phys. Rev. D **82**, 054502 (2010); A. Li, A. Alexandru, and K. F. Liu, arXiv:1103.3045.
- [49] J. Braun, L. M. Haas, F. Marhauser and J. M. Pawłowski, Phys. Rev. Lett. **106**, 022002 (2011).
- [50] Y. Sakai, K. Kashiwa, H. Kouno and M. Yahiro, Phys. Rev. D **77**, 051901(R) (2008).
- [51] K. Morita, V. Skokov, B. Friman, and K. Redlich, arXiv:1107.2273.
- [52] A. Roberge and N. Weiss, Nucl. Phys. B **275**, 734 (1986).
- [53] Y. Sakai, K. Kashiwa, H. Kouno, and M. Yahiro, Phys. Rev. D **78**, 036001 (2008); Y. Sakai, K. Kashiwa, H. Kouno, M. Matsuzaki, and M. Yahiro, *ibid.* **78**, 076007 (2008); *ibid.* **79**, 096001 (2009)
- [54] K. Kashiwa, T. Hell, and W. Weise, arXiv:1106.5025.
- [55] V. Pagura, D. Gómez Dumm, and N. N. Scoccola, arXiv:1105.1739.
- [56] C. Wetterich, Phys. Lett. B **301**, 90 (1993).
- [57] T. R. Morris, Int. J. Mod. Phys. A **9**, 2411 (1994).
- [58] U. Ellwanger, Z. Phys. C **62**, 503 (1994).
- [59] J. Berges, N. Tetradis and C. Wetterich, Phys. Rept. **363**, 223 (2002).
- [60] B. J. Schaefer and J. Wambach, Phys. Rev. D **75**, 085015 (2007).
- [61] B. Stokic, B. Friman and K. Redlich, Eur. Phys. J. C **67**, 425 (2010).
- [62] V. Skokov, B. Stokic, B. Friman and K. Redlich, Phys. Rev. C **82**, 015206 (2010)
- [63] K. Fukushima, Phys. Rev. D **77**, 114028 (2008) [Erratum-*ibid.* D **78**, 039902 (2008)]
- [64] B. J. Schaefer, M. Wagner and J. Wambach, Phys. Rev. D **81**, 074013 (2010)
- [65] D. U. Jungnickel and C. Wetterich, Phys. Rev. D **53**, 5142 (1996).
- [66] L. F. Palhares and E. S. Fraga, Phys. Rev. D **78**, 025013 (2008); E. S. Fraga, L. F. Palhares and M. B. Pinto, Phys. Rev. D **79**, 065026 (2009)
- [67] V. Skokov, B. Friman, E. Nakano, K. Redlich and B. J. Schaefer, Phys. Rev. D **82**, 034029 (2010)
- [68] E. Nakano, B. J. Schaefer, B. Stokic, B. Friman and K. Redlich, Phys. Lett. **B682**, 401 (2010).
- [69] V. Skokov, B. Friman and K. Redlich, Phys. Rev. C **83**, 054904 (2011).